Medium-chain fatty acid and its derivative impact mucus properties and vary with age and gestational maturity

International Journal of Biological Macromolecules 381 (2026) 154076

Contents lists available at ScienceDirect

International Journal of Biological Macromolecules

journal homepage: www.elsevier.com/locate/ijbiomac

Medium-chain fatty acid and its derivative impact mucus properties and vary with age and gestational maturity

J.S. Mortensen [a], L.S. Krog [a], S.S.-R. Bohr [a,b], L. Råberg [c], A. Stubelius [c], L. Saaby [d], N.S. Hatzakis [b], D.N. Nguyen [e], S. Rønholt [a], H.M. Nielsen [a,*]

[a] Center for Biopharmaceuticals and Biobarriers in Drug Delivery (BioDelivery), Department of Pharmacy, Faculty of Health and Medical Sciences, University of Copenhagen, Universitetsparken 2, DK-2100, Copenhagen, Denmark
[b] Department of Chemistry, Faculty of Science, University of Copenhagen, Thorvaldsensvej 40, DK-2100, Copenhagen, Denmark
[c] Department of Life Sciences, Division of Chemical Biology, Chalmers University of Technology, Sweden
[d] Bioneer A/S, Kogle Alle 2, DK-2970, Hørsholm, Denmark
[e] Department of Veterinary and Animal Science, Faculty of Health and Medical Sciences, University of Copenhagen, Grønnegårdsvej 15, DK-1870, Frederiksberg, Denmark

ARTICLE INFO

Keywords:
Glycoprotein sialic acid
Single particle tracking
Decanotate, Salcaprozate

ABSTRACT

The intestinal mucus is a critical component of human health, acting as the first line of defense against pathogens. Yet, mucus has been reported to be more permeable and thus less of a barrier to pathogens both earlier and later in life. Lipids and their digestion products, such as medium-chain fatty acids (MCFAs), can strengthen the mucus barrier thereby reducing pathogen diffusion. Herein, the diffusion of a pathogen marker in *ex vivo* porcine intestinal mucus decreased with increasing pig age (5-day to 4-month) and gestational immaturity (term vs preterm). Upon the addition of the MCFA sodium decanoate (C10) as well as salcaprozate sodium (SNAC), an MCFA derivative, mucus' viscosity increased ≥7-fold and, importantly, the pathogen marker diffusion in the mucus decreased significantly. Interestingly, this effect was substantially more pronounced in mucus from older and from gestationally immature pigs. Relevant physicochemical properties of mucus (osmolality, protein and sialic acid contents) changed depending on the age and gestational maturity of the donor pigs. Notably, we found that cleavage of mucin-bound sialic acids resulted in a 3–4-fold lower effect of C10 and SNAC on mucus viscosity, establishing a direct link between the mucin-bound sialic acid and mucus' interaction with the MCFA and derivative. Overall, these findings demonstrate that the properties of the mucus barrier and the protective effects lipids like MCFAs are highly influenced by age and gestational maturity. Therefore, our results highlight the need for nutrition and therapeutic strategies tailored to specific age periods to ensure optimal gut health.

1. Introduction

The intestinal mucus barrier safeguards the intestinal epithelium by delicately balancing the effective passage of nutrients, while entrapping and restricting the passage of harmful molecules and pathogens [1]. Interestingly, mucus is a dynamic barrier with properties changing depending on health and disease, as well as with age [1–8]. However, these biological changes are rarely accounted for when assessing interactions of e.g. pharmaceuticals or nutritional compounds' effect on the mucus barrier.

Mucus is a highly viscous gel, generally composed of mainly water, low amounts of mucins and lipids, and minute amounts of proteins, DNA, electrolytes and cell debris [9,10]. While mucins are generally considered the structural component of mucus, lipids are equally important for the structural integrity of mucus [11–13]. Interestingly, food-related stimuli, such as the introduction of exogenous lipids and their digestion products, have been reported to reinforce the mucus barrier, reducing the diffusion of pathogens and model markers of these within the mucus [14–17]. We recently reported that the addition of sodium decanoate (C10), a common medium-chain fatty acid (MCFA) product from digestion of triglycerides and also found in bovine milk and infant formulas [18–20], significantly reduced the diffusion of nanoparticles, used as a pathogen marker, in intestinal mucus from piglets that experienced perinatal hypoxia at birth [3]. Perinatal

* Corresponding author at: Universitetsparken 2, 2100, Copenhagen, Denmark.
E-mail address: hanne.morck@sund.ku.dk (H.M. Nielsen).

https://doi.org/10.1016/j.ijbiomac.2026.154076
Received 26 March 2026; Received in revised form 23 June 2026; Accepted 13 August 2026
Available online 16 August 2026

hypoxia is a major risk factor for necrotizing enterocolitis [21,22], a severe inflammatory condition associated with high mortality [23,24]. Interestingly, we further observed that the impact of C10 on pathogen marker diffusion in mucus varied markedly with these piglets' health status and gestational maturity [3,25]. Hence, other biological factors such as age of the animal may also affect the protective mucosal nature of C10. Beyond their role in improving the intestinal mucus barrier in piglets, MCFAs have emerged as promising interventions for enhancing neonatal survival [25,26] and for managing metabolic disorders [27], underscoring the need to better understand how MCFAs influence the intestinal mucus barrier following administration.

While C10 is a common food additive with no consumption limit specified [28–30], C10 in high doses is also extensively studied in the pharmaceutical industry and research to enhance the permeation of peptide and protein drugs through the gastrointestinal mucosa [31–33]. An MCFA derivative, salcaprozate sodium (SNAC), was also shown to be able to increase oral absorption of the GLP-1 analog semaglutide, an anti-diabetic and anti-obesity drug, paving the way for the first semaglutide tablet on the market [33–35]. Yet, using the *ex vivo* porcine intestinal mucus model, PIM, Twarog et al. found that both SNAC and C10 at 100 mM significantly increased the viscosity of PIM 15-fold and 7-fold at a low shear rate of 0.01 s^{-1}, respectively [36]. We reported a similar increase in viscosity of PIM with 150 mM SNAC, which was further associated with reduced nanoparticle diffusion and permeation of the peptide cyclosporine A and of the protein ovalbumin through PIM in the presence of SNAC [37]. This suggests that both C10 and SNAC may strengthen the intestinal mucus barrier rather than act as mucus permeation enhancers to facilitate peptide absorption. Understanding how MCFAs and derivatives interact with and affect the intestinal mucus barrier may aid future design of both oral drug delivery excipients and of therapeutic and nutritional strategies for inflammatory gut diseases characterized by mucus barrier dysfunction, including necrotizing enterocolitis, Crohn's disease, and ulcerative colitis [3,5,8,38].

The barrier properties of intestinal mucus are dynamically changing with age, becoming less permeable to *Escherichia coli* and nanoparticles from the infant state towards adulthood (5- vs 21- day old rat pups [2]; 5- vs 9- vs 19-day old pigs [3]; 14-day vs 7–19-month old pigs [4]). Also, the chemical composition of mucus, e.g. DNA content [4] and mucin content [7,39] as well as genes responsible for the mucin synthesis and post-translational modification of mucin glycosylation have been reported to change with age, resulting in a higher degree of acidic glycans (e.g. content of sialic acids (SA)) after weaning in all mammalian species, including humans [2,3,40]. As the mucin structure and the chemical composition of mucus define the overall barrier properties of mucus [9,41–47], differences in age may affect how compounds such as, but not limited to, MCFAs and derivatives interact with and affect mucus barrier properties.

By applying rheological and single particle tracking (SPT) measurements, we aimed to investigate how the MCFA, C10, and an MCFA derivative, SNAC, affected the barrier properties of intestinal mucus from pigs of different ages and gestational maturities. Additionally, we aimed to evaluate if any age or gestational maturity differences in mucus' interaction with the components were related to different physicochemical properties of the mucus samples.

2. Materials and methods

2.1. Materials

Sodium 8-[(2-hydroxybenzoyl)amino]octanoate (salcaprozate sodium, SNAC) (> 99%) and sodium decanoate (sodium caprate, C10) (> 99%) were obtained from EzBiolab (Shanghai, China) and Tokyo Chemicals Industry Co. (Tokyo, Japan), respectively. Acetic acid glacial (Ph. Eur., USP) and Hank's Balanced Salt Solution (HBSS, with calcium, magnesium, bicarbonate, and without phenol red) were purchased from VWR (Søborg, Denmark). MES anhydrous BioChemica (MES) was obtained from PanReac AppliChem (Darmstadt, Germany). Schiff's reagent for aldehydes (Schiff's reagent), bovine serum albumin (BSA) (> 98%), 1 g/dL periodic acid solution, 5 U neuraminidase (sialidase) from *Clostridium perfringens* (Roche), Sialic Acid Assay Kit and mucin from porcine stomach type II (PGMII) were obtained from Sigma-Aldrich (Søborg, Denmark). SPHERO™ fluorescent Nile red polystyrene particles with a diameter of 100–300 nm (NP) were obtained from Nordic BioSite (Copenhagen, Denmark). GentleMACS™ M tubes were obtained from Miltenyi Biotec (Lund, Sweden). RNeasy Mini kit and DNase kits were purchased from Qiagen (Hilden, Germany). Acetic acid (99–100%), Pierce™ BCA protein assay kit and High-Capacity cDNA Reverse Transcription Kit were obtained from Fisher Scientific (Roskilde, Denmark). LightCycler® 480 SYBR Green I Master was purchased from Roche Diagnostics (Hvidovre, Denmark). PrimePCR™ SYBR® Green Assay *MUC5AC* from pig was obtained from Bio-Rad (Copenhagen, Denmark). Primers for *MUC1, MUC2, GAPDH and HPRT1* were designed using Primer-Blast (Primer-BLAST: http://www.ncbi.nlm.nih.gov/tools/primer-blast/) with sequences listed in Supplementary Material, Table S1.

2.2. Collection of ex vivo porcine intestinal tissue and mucus

Surplus small intestines were obtained either from healthy pigs (Danish Landrace x Yorkshire x Duroc) used for surgical training (3–4-month old, fasted) or for experimental studies (5–19-day old) either farrowed at gestation day ~117 (term), delivered via caesarean section at gestation day 113 (term) or delivered via caesarean section at gestation day 106 (preterm). For an overview of the different pigs and litters used for the different experiments, see Supplementary Material, Table S2. Immediately after euthanasia, the small intestines were isolated. Tissue samples of similar sizes (5–10 cm) for real-time quantitative polymerase chain reaction (qPCR) analysis were collected just distal to Treitz ligament (proximal sample) and proximal to cecum (distal sample). These tissue samples were gently squeezed to remove food content and transferred to cryo-tubes prior to snap-freezing in liquid nitrogen and storage at −80 °C until analysis. The remaining intestine samples were used for mucus collection, with the procedure described in [37]. Mucus from individual pigs were pooled, aliquoted, and stored at −20 °C until analysis. For the 3- and 4-month old pigs, only up to 8 m of the proximal small intestine was used for mucus collection, while for the 5–19-day old pigs the entire small intestine was used. To minimize degradation of the biologic material, intestines and mucus were always kept on ice during the isolation procedure. Intestines were handled according to the authorization for the use of animal by-products and derived products for research and diagnosis approved by the Danish Veterinary and Food Administration (license number DK-13-oth-931,833).

2.3. Rheological investigations of mucus

Prior to investigation, mucus was thawed overnight in the fridge (~4 °C) and was hydrated using 10 mM MES in HBSS pH 6.5 (mHBSS) (71.4% mucus to 28.6% mHBSS (v/v)) just before the measurement. Hydrated mucus was added to tubes containing C10 or SNAC powder and mixed for final concentrations of 25, 50, 75 mM C10 or 50, 100, 150 mM SNAC in mucus. After 1 h of incubation at 37 °C, the sample was loaded on the Peltier plate of an AR-G2 rheometer equipped with a 40 mm 1° truncated cone and a solvent trap (TA Instruments-Waters, New Castle, DE, USA). Rheological measurements were conducted as previously described [37].

For rheological measurements of mucus pellets from the neuraminidase study (Section 2.10.), pellets were thawed and stored at 4 °C alone or supplemented with 150 mM C10 or SNAC for a minimum of 1 h before measurements. Rheological measurements of the mucus pellets were conducted similarly to the hydrated mucus samples, except that the measurements were conducted at 20 °C to avoid sample evaporation and

that ranges of 0.01–100 s^{-1} over 20 min and 0.01–1000 Pa were used for the continuous flow ramp and the stress sweep to match the mucus pellets rheological ranges, respectively.

Of the full rheological dataset (Supplementary Material, Fig. S1 and S2) the viscosities at a biologically relevant shear rate of 0.4 s^{-1} [48], the stress stability (yield and flow point) as well as the storage modulus (G′) and the storage factor (i.e. ratio between G′/G″) at 1 rad/s were used for rheological evaluation. The yield point obtained from the stress sweep was determined as the oscillation stress value where the storage modulus G′ declined by a maximum of 5% from the mean of minimum five data points (G′) within the linear area. The flow point was also obtained from the stress sweep and determined as the first oscillation stress value where the G′/G″ ratio was below 1.

2.4. Cryo-scanning electron microscopy (cryo-SEM) of mucus

A small amount of hydrated mucus (71.4% mucus to 28.6% mHBSS (v/v)) alone or incubated with C10 or SNAC (final concentration of 50 mM) for 1 h was used for cryo-SEM, as previously described in [37]. Image analysis of 12–15 cryo-SEM images of representative samples for each condition was performed in MATLAB® R2021b (MathWorks, Natick, MA, USA). The utilized code is listed in the Supplementary Information Table S3.

2.5. Single particle tracking in mucus

Diffusion of fluorescent Nile red 100–300 nm nanoparticles (NPs) in the absence or presence of C10 or SNAC in mucus was investigated by single particle tracking as previously described [37]. Briefly, mucus was hydrated and vortexed with mHBSS alone or mHBSS containing C10 or SNAC. Samples were incubated at 37 °C for 1 h prior to the addition of NPs. The final hydration level of mucus was 71.4% mucus to 28.6% mHBSS (*v*/v) with 50 mM C10 or 50 mM SNAC and 0.08 mg/mL NPs. Each sample was applied to a microscope glass slide placed in a custom-built Teflon microscope chamber. Image time series were acquired at 37 °C using an inverted spinning disk confocal microscope (Olympus SpinSR10, Olympus, Tokyo, Japan) equipped with a 60× oil immersion objective with a numerical aperture of 1.4 (Olympus) and a CMOS camera (Photometrics PRIME 95B, Teledyne Photometrics, Tucson, AZ, USA) with a pixel dimension of 0.183 × 0.183 μm. Measurements were recorded at a frequency of 166.66 Hz using laser excitation at a wavelength of 532 nm. Quantitative analysis of the motion of all NPs was conducted using our previously published methodologies [49–51] for robust spot detection and trajectory linking. To ensure adequate biological data collection, each biological replicate consisted of 5–10 measurements (i.e. for each *N*, $n = 5–10$), which were pooled to constitute the dataset for each biological sample. By analyzing the behavior of individual NPs, ensemble averaging was circumvented, providing increased resolution towards understanding how the C10 or SNAC changed the NPs movement in mucus. For each trajectory, the diffusion coefficient was calculated as previously demonstrated [50,52,53] by fitting all displacements to the probability density function (under the assumption that movement is Brownian) using an unbinned maximum likelihood. The density function is given by Eq. (1):

$$p(r,t,D) = \frac{r}{2Dt} \bullet e^{\frac{r^2}{4Dt}} \quad (1)$$

where r is the observed NP displacement between consecutive frames, t is the acquisition time (6 ms) and D is the diffusion coefficient. This method was chosen over the more classical mean square displacement (MSD) analysis as it is less susceptible to bias from short trajectories. However, recognizing the strength of MSD analysis to capture potential trapping, NPs were investigated using the anomalous diffusion parameter that directly describes particle confinement. To extract this information, Eq. (2) for two dimensions was used:

$$MSD = 4Dt^{a} \quad (2)$$

where D is the instantaneous diffusion coefficient, t is the time lag, and α is the anomalous diffusion parameter. Based on careful inspection of our data and previous results [37], NPs were categorized as immobile for $\alpha < 0.001$, confined $0.001 < \alpha < 0.5$, or freely moving $0.5 < \alpha$.

As a further validation, the apparent NP spread using a 2D heatmap of NP coverage was provided. In short, this is made by setting all starting positions to the same coordinates and quantifying how NPs move away from their origin.

2.6. MUC gene expression in intestinal tissue

Gene expression of the target genes; *MUC1, MUC2, MUC5AC,* and references, the housekeeping genes; *GAPDH and HPRT1*, in the proximal and distal part of the small intestines were determined by qPCR. RNA was isolated and purified from homogenized intestinal tissue with the commercial RNeasy Mini kit and DNase kit according to the manufacturer's protocol with additional rinsing steps to improve RNA purity. The changes to the manufacturer's protocol were as follows: after loading the sample to an RNeasy Mini Spin column, the sample was washed 2× with 350 μL RW1 buffer and centrifuged at 10,000 ×*g* for 1 min before doing on-column DNase digestion at room temperature for 15 min. After incubation, the column was washed 1× more with 350 μL RW1 buffer and centrifuged at 10,000 ×*g* for 1 min. Hereafter, the column sample was washed 2× with 500 μL RPE buffer and centrifuged at 10,000 ×*g* for 1 min before a final wash with 500 μL RPE buffer and centrifugation at 10,000 ×*g* for 3 min. To ensure that the washing buffers were properly removed from the samples, the column was centrifuged dry at 20,000 ×*g* for 3 min. The RNA was eluted with RNase-free water and the concentration and purity of isolated RNA was measured at 230, 260/280 nm, respectively. Purified RNA concentrations ranged between 330 and 1966 ng/μL, the 260/280 ratio between 2.06 and 2.13, and the 260/230 ratio between 1.96 and 2.26, meaning that the samples were free from impurities. 0.2 μg/μL of RNA was then converted into cDNA with a commercial High-Capacity cDNA Reverse Transcription Kit according to manufacturer's instructions. Using a LightCycler 480 system (Roche, Basel, Switzerland) with the commercial qPCR kit (LightCycler® 480 SYBR Green I) gene expression was determined. Samples were analyzed in duplicates with a maximum accepted variation of 2.5% of the Cp-values of all genes. If the variation in Cp-values was greater than 2.5% or more than one peak in the melting was observed, samples were either re-analyzed and/or excluded. All procedures were performed at 4 °C on ice if not otherwise stated. Gene expression was given as fold changes relative to expression levels of the references *GAPDH* and *HPRT1* according to Eq. (3).

$$\text{Relative gene expression} = \frac{2^{-Cp_{\text{target gene}}}}{2^{-\text{geomean}(Cp_{GAPDH}, Cp_{HPRT1})}} \quad (3)$$

2.7. Glycoprotein content in mucus

The glycoprotein content in mucus collected from pigs at different ages and maturities was determined by a colorimetric assay with periodic acid-Schiff staining (PAS) based on previous reports [54,55]. Mucus was diluted 30× in demineralized water and technical triplicates of 25 μL demineralized water, PGMII standard (0.5–6 mg/mL), or diluted mucus were pipetted into clear-bottom 96-well plates (Greiner, Th. Geyer Skandinavien ApS, Ballerup, Denmark). To each well, 120 μL of 0.06% (v/v) periodic acid solution and 7% (v/v) acetic acid in demineralized water was added. The 96-well plate was incubated for 90 min at 37 °C after which the plate was cooled to room temperature (10 min) before adding 100 μL Schiff's reagent to each well. The plate was incubated at room temperature for another 40 min before measuring absorbance at λ = 562 nm using a plate reader (FLUOstar Omega, BMG LABTECH, Ortenberg, Germany).

2.8. Protein content in mucus

The protein content in mucus was determined using the commercial Pierce™ BCA protein assay kit as previously described [56]. BSA standards ranged between 0.1 and 0.8 mg/mL and 500× diluted mucus samples were used for analysis. The absorbance at λ = 562 nm was measured with a plate reader (FLUOstar Omega).

2.9. Sialic acid (SA) content in mucus

The total and free SA (TSA and FSA, respectively) content in mucus was determined by using the commercial Sialic Acid Assay Kit according to the manufacturer's protocol. Briefly, mucus samples were diluted 1:1 (v/v) with ultrapure water and vortexed. For TSA determination, technical triplicates of 20 μL diluted mucus were hydrolyzed with 80 μL of the hydrolysis mix for 60 min at 80 °C before being precipitated with 25 μL 10% (v/v) TCA and centrifuged at 16,000 ×*g* (Microcentrifuge, Eppendorf SE, Hamburg, Germany) for 10 min. After centrifugation, 25 μL of the supernatant was transferred to a new tube for color reaction. For FSA determination, technical triplicates of 40 μL diluted mucus were mixed with either 10 μL 10% (v/v) TCA or 10 μL ultrapure water and centrifuged at 16,000 ×*g* for 10 min. 25 μL of the supernatant was transferred to a new tube for color reaction. For the standard curve samples (50–500 μM SA), 20 μL of the sample was mixed with 5 μL 10% (v/v) TCA directly in the tube for the color reaction. For the color reaction, 125 μL of the working reagent was added to a 25 μL supernatant sample and incubated for 60 min at room temperature. After incubation, 50 μL of the dye reagent was added to each sample and the samples were heated for 10 min at 100 °C, after which 100 μL DMSO was added to each sample and centrifuged at 16,000 ×*g* for 5 min. Then, 200 μL of the supernatant was transferred to a clear 96-well plate (Greiner, Th. Geyer Skandinavien ApS) and the absorbance at λ = 549 nm was measured using a plate reader (HIDEX Sense, Hidex Oy, Turku, Finland).

2.10. Neuraminidase treatment of mucus

To assess the role of terminal SA units attached to mucins for the interaction between mucus and C10 or SNAC, mucus was treated with a neuraminidase, cleaving the terminal SA residues of α2,3-, α2,6-, or α2,8-linked to Gal, GlcNAc, GalNAc, AcNeu, GlcNeu, oligosaccharides, glycolipids, or glycoproteins. For optimal treatment of mucus with the neuraminidase and removal of cleaved SA before rheological studies, different dilutions of mucus, neuraminidase concentration, incubation time, and centrifugation condition were investigated (Supplementary Material, Fig. S3). The final protocol included that mucus was thawed and diluted 3× in ice-cold 100 mM acetate buffer pH 5.0 (acetate buffer) and vortexed for 10–15 s. The pH was then adjusted to pH 5.0 with 5 M HCl. The 3× diluted mucus sample was subsequently either further diluted with acetate buffer (untreated preparation) or with neuraminidase at a final concentration 100 mU/mL (treated preparation) to reach a final 4× dilution of the mucus. The untreated preparation was further divided into two types of preparations: Untreated÷ (i.e. untreated mucus preparation without incubation) and untreated-incubated (i.e. untreated mucus preparation with incubation at 37 °C). After preparing the untreated÷, untreated-incubated, and neuraminidase-treated preparations, samples for TSA and FSA determination were collected (i.e. 0 h sample*)*. Immediately thereafter, the untreated÷ preparation was centrifuged at 2000 ×*g* (LLG-uniCFUGE 3 pro, LLG-labware, Hambuch, Germany) for 1 min and TSA and FSA samples were taken from both the supernatant and pellet samples. The untreated-incubated and neuraminidase-treated mucus preparations were incubated for 2 h at 37 °C, after which TSA and FSA samples were taken (i.e. 2 h sample). The untreated-incubated and neuraminidase-treated mucus preparations were then further centrifuged at 2000 ×*g* (LLG-uniCFUGE 3 pro, LLG-labware) for 1 min, whereafter samples for TSA and FSA were collected from both supernatants and pellets. The pellets were saved for further rheological measurements. All TSA, FSA, and pellet samples were immediately frozen at −20 °C until SA determination and rheological measurement (as described above), respectively.

2.11. Statistics

Statistical analysis of data was performed with GraphPad Prism 10.4 from GraphPad Software Inc. (La Jolla, CA, USA). Student's *t*-test or a one-way analysis of variance (ANOVA) followed by a Dunnett's comparisons test (for comparison to the control condition) or a Tukey's multiple comparisons test (for comparison between all conditions) was used for statistical hypothesis testing between two or more means, respectively. Differences were considered statistically significant if $p < 0.05$. A Welch test was used in the case of unequal variance based on either an F-test or a Brown-Forsythe test. Biological replicates, i.e. mucus from different pigs, are indicated with ***N***, while ***n*** states the number of technical replicates performed for each biological sample.

3. Results

3.1. The viscoelastic properties of mucus changed in a concentration-dependent manner in the presence of C10 or SNAC with as little as 50 mM needed for significant alterations

The MCFA, C10 and the MCFA derivative, SNAC, share some structural similarities, both having a carboxylic acid group (pKa ~ 5.0) anchored to a saturated lipid chain of 10- or 8-carbon chains, respectively. In addition, SNAC has a terminal hydroxybenzoyl group, increasing the hydrophilicity of SNAC compared to that of C10 [57]. As both C10 and SNAC have been reported to change the viscoelastic properties of mucus [36,37], we employed rheology to establish at which concentrations C10 and SNAC would interact with as well as how they would affect the viscoelastic properties of mucus.

By applying C10 and SNAC to mucus at relevant concentrations [34,58–62]; i.e. reflecting physiologically plausible local intestinal concentrations following dissolution from an orally administered dosage form [63–65], we observed that both C10 and SNAC induced concentration-dependent increases in the G′ and viscosity of mucus, indicating an increased number of, and/or strengthened intermolecular interactions within the mucus network [3,66]. In contrast, both the storage factor and stress stability of mucus did not show any concentration-dependent effect for SNAC presence, whereas increasing the C10 concentration tended to lead to a reduction in both parameters reaching levels to that of mucus alone (Fig. 1B and D). These findings suggest that high C10 concentrations increase the stiffness of the mucus gel, while SNAC, particularly at high concentrations, predominantly strengthens the mucus network.

At 50 mM, the presence of C10 or SNAC increased G′ of mucus by 16-fold and 32-fold, respectively (Fig. 1A), with corresponding significant increases in viscosity (Fig. 1C). Although SNAC tended to exert stronger effects across all rheological parameters (1.1–2.0-fold) than C10, no statistically significant differences were observed between the 50 mM conditions by *t*-test evaluations. The presence of C10 and SNAC both increased mucus pH and osmolality in a concentration-dependent manner, with comparable levels at 50 mM (Supplementary Material, Table S4). Overall, a minimum concentration of 50 mM C10 or SNAC was required to significantly increase G′ and the viscosity of mucus.

3.2. C10 and SNAC increase confinement of the pathogen marker in mucus with effects more pronounced in older and immature pigs

The vital capability of mucus to entrap and clear pathogens is essential to maintain mucosal homeostasis. Yet, in early life, the mucus barrier is reported to be more susceptible to pathogen penetration compared to later in life [2–4], likely due to a more loose mucus microstructure [4]. Indeed, we observed a more loosely structured

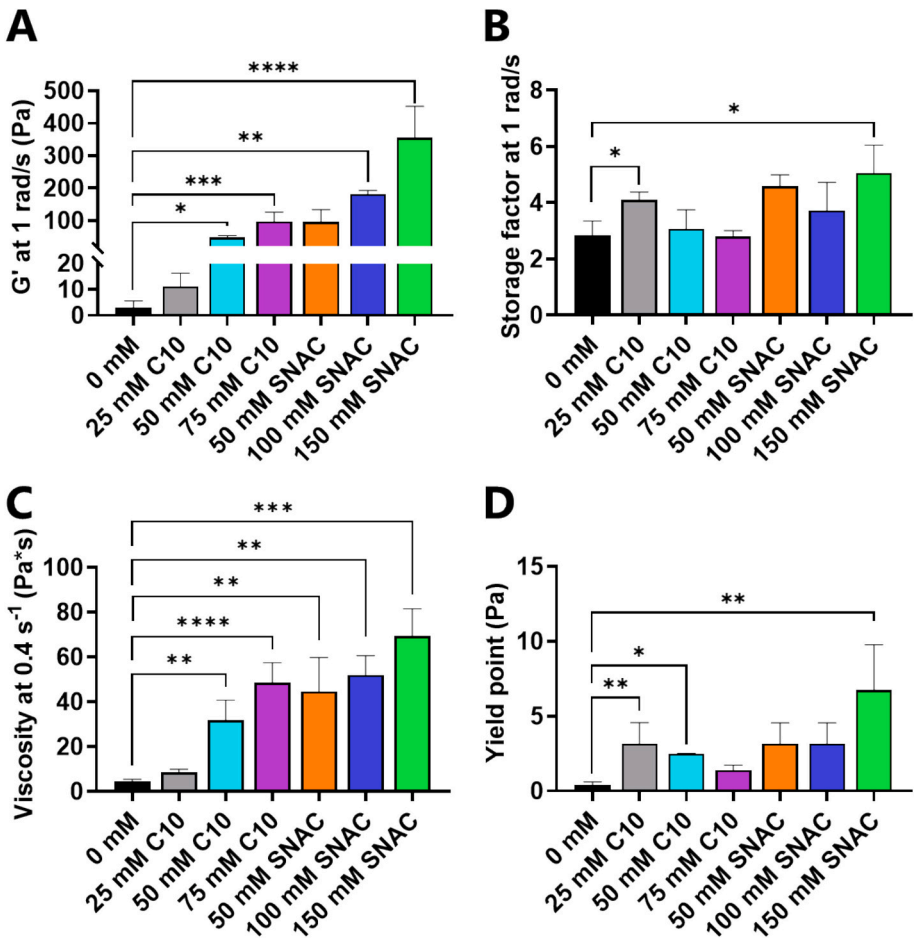

Fig. 1. Viscoelastic properties of *ex vivo* porcine small intestinal mucus collected from 3-month old pigs in the absence and in the presence of sodium decanoate (C10) and sodium 8-[(2-hydroxybenzoyl)amino]octanoate (SNAC). A) storage modulus (G′) at 1 rad/ s, B) ratio of storage G′ vs loss modulus G″ (storage factor) at 1 rad/s, C) viscosity at 0.4 $s_{,}^{-1}$ and D) end of the linear viscoelastic region (yield point) of mucus in the absence (black) and in the presence of 25 mM C10 (grey), 50 mM C10 (turquoise), 75 mM C10 (purple), 50 mM SNAC (orange), 100 mM SNAC (blue), and 150 mM SNAC (green). Data are given as means of biological replicates with standard deviation of $N = 3$–4, $n = 1$–3. Data were statistically different from the 0 mM condition for the C10 or SNAC group as stated by * ($p < 0.05$), ** ($p < 0.01$), *** ($p < 0.001$) or **** ($p < 0.0001$). (For interpretation of the references to color in this figure legend, the reader is referred to the web version of this article.)

mucus in the younger pigs (9- and 19-day) compared to that in the older pigs (3- and 4-month) (Fig. 2A and Supplementary Material, Fig. S4). In contrast, the microstructure of mucus from the preterm pig appeared denser than that of the term pig. Interestingly, upon the addition of either 50 mM C10 or SNAC, the microstructure of mucus in most cases tended to become denser, with smaller pores, though the microstructure for all conditions appeared very heterogeneous without any clear trends related to the donor pig age or gestational maturity.

Analysis of the cryo-SEM images assessed microstructural changes in terms of pore size, number of pores, and pore wall density (Fig. 2B–C; Fig. S5–7). Due to the heterogeneity of mucus and the high variability in pore size, mean and median pore size were identified as not reliable descriptors. Instead, numbers of pores and pore wall density were used, as they showed lower variance and enabled clearer detection of PE-induced effects.

For the 3-month and 5-day old pigs, C10 or SNAC exposure increased the number of pores in the mucus (i.e. decreased pore size) compared to the control (Fig. 2B). In contrast, mucus from 4-month, 19-day, and 5-day old preterm pigs showed either no change or up to a 50% decrease in pore number. The pore wall density trends largely followed those of pore number (Fig. 2C), except for the 5-day old term and preterm pigs, where opposite tendencies were observed, suggesting that PE-induced changes in the pore wall thickness in these groups. Along with the clear effect of the PE obtained by image analysis, it should be noted that these observations are based on a single biological replicate and therefore should be interpreted with caution.

To assess the age-dependent effects of C10 and SNAC on mucus, 100–300 nm fluorescent NPs were added to the mucus samples, and the trajectories of individual NPs were tracked. This allowed us to directly observe the spatiotemporal localization of individual NPs [37,50], gaining insights into their movement within mucus and hence the microstructural effect of C10 and SNAC. The NPs were used as a pathogen marker as the NP size range is comparable to that of pathogenic microbes [67]. From individual trajectories, the spatial coverage of a considerable number of NPs (885–13,384 particles) was quantified and visualized as average coverage plots (Fig. 3A). In addition, the anomalous diffusion exponent (α) was calculated to assess the degree of NP confinement within the mucus (Fig. 3C, Supplementary Material, Fig. S8).

In mucus alone (0 mM), both the average coverages in which the NPs moved and the fractions of freely moving NPs (i.e. exhibiting movement like that in buffer) tended to decrease slightly with increasing age and gestational immaturity (Fig. 3A and C). When either 50 mM C10 or SNAC was present in the mucus, the coverage of the NPs tended to decrease in all mucus samples, most likely in response to increased NP confinement (Fig. 3A and C). This suggests that the presence of C10 or SNAC may reduce microbial penetration in mucus.

Interestingly, while C10 and SNAC induced the same degree of NP confinement within individual mucus groups ($p > 0.05$), this effect was more pronounced in mucus from the older pigs and the immature pigs

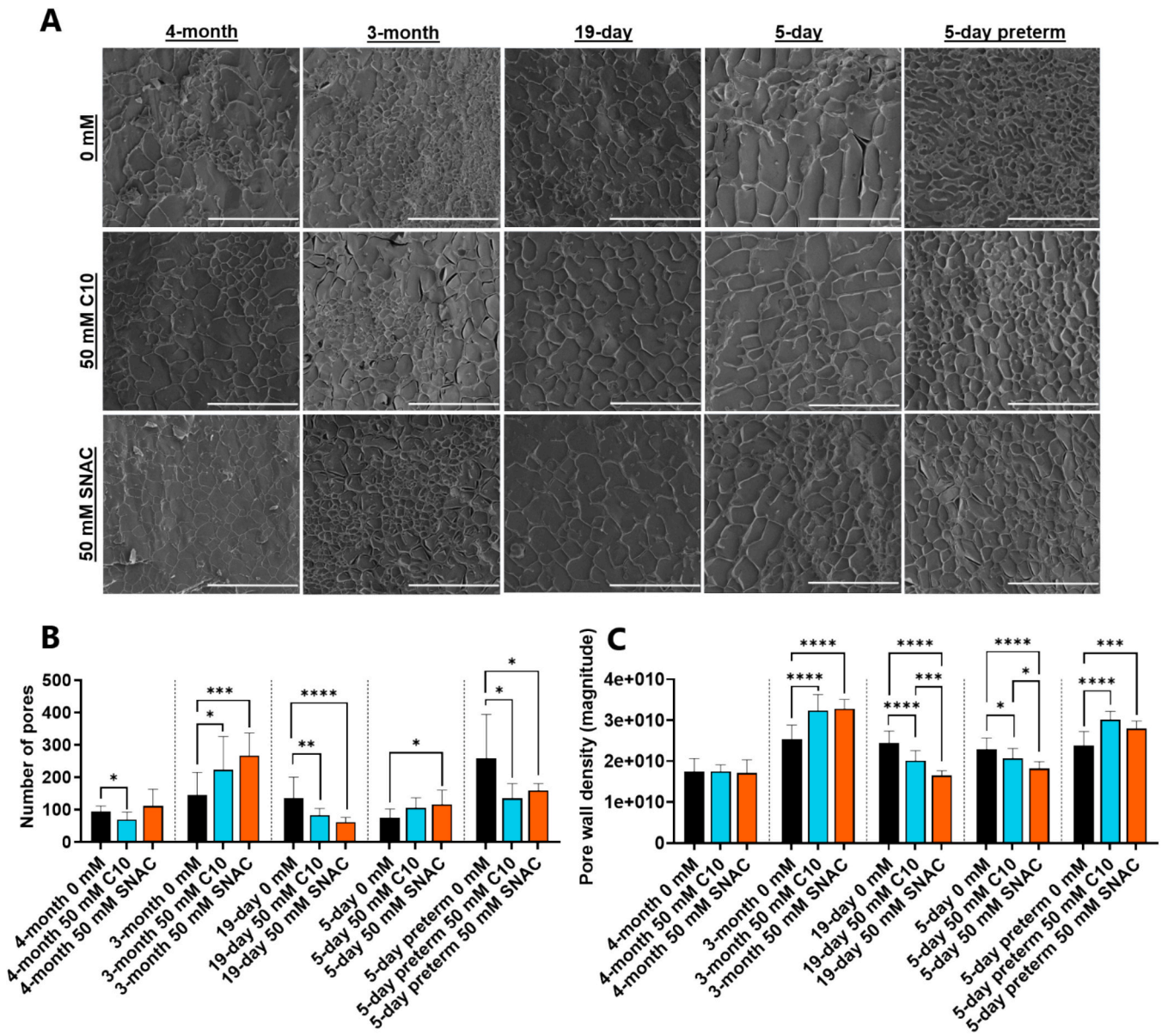

Fig. 2. Visual appearance, pore size and pore wall analysis of *ex vivo* porcine small intestinal mucus (PIM) collected from pigs at different age and gestational maturity (i.e. 4-month, 3-month, 19-day, 5-day, and 5-day preterm pigs) in the absence and the presence of either 50 mM sodium decanoate (C10) or 50 mM sodium 8-[(2-hydroxybenzoyl)amino]octanoate (SNAC). A) representative cryo-scanning electron microscopy images of PIM with scale bars of 20 μm. B) number of pores and C) pore wall density of PIM based on image analysis. Data are given as mean with standard deviation of $N = 1$, $n = 12$–15. Statistical difference between PIM in the absence and in the presence of C10 or SNAC was detected as indicated by * ($p < 0.05$), ** ($p < 0.01$), *** ($p < 0.001$), or **** ($p < 0.0001$).

(Fig. 3C). Here, the presence of C10 and SNAC reduced the fraction of freely moving NPs in mucus to a negligible number (<3%), by 7–98-fold, 17–98-fold and 102–134-fold, for 4-month, 3-month, and 5-day old preterm pigs, respectively. In contrast, 16–23% freely moving NPs were still present in mucus from the 19- and 5-day old pigs, although the fraction of freely moving NPs still decreased 2–4-fold in the presence of C10 or SNAC. In addition to increased NP confinement in mucus, the presence of C10 and SNAC also decreased the diffusion coefficient of the NPs within the mucus by 25–100%, except for the 3-month old pigs. Also, for this parameter, the effects of C10 and SNAC tended to be more pronounced for the older and the immature pigs (Fig. 3B and Supplementary Material, Fig. S9), whereas the diffusion coefficients in mucus alone (i.e. 0 mM) tended to be independent of pig age and gestational maturity (Fig. 3B).

While cationic compounds can be trapped and confined in mucus due to charge interaction with the negatively charged mucins [9,15], this was not the case for the NPs, as the presence of C10 (−39.8 ± 1.7 mV) or SNAC (−49.4 ± 2.4 mV) only further decreased the zeta-potential of the NPs compared to that in buffer (−29.1 ± 2.2 mV).

Overall, the addition of C10 or SNAC to mucus from pigs of all ages and maturities markedly slowed and confined NP movement, suggesting that C10 and SNAC may reduce pathogen penetration in mucus. While the effect of C10 and SNAC on diffusion was similar within the same mucus group, their effect on mucus was strongly dependent on the age and gestational maturity of the donor pig.

3.3. Physicochemical properties of mucus differ depending on pig age and gestational maturity

Physicochemical properties of mucus are known to govern how mucus interacts with exogenous compounds such as MCFAs [9,43]. Hence, we next sought to determine the pH, osmolality, protein,

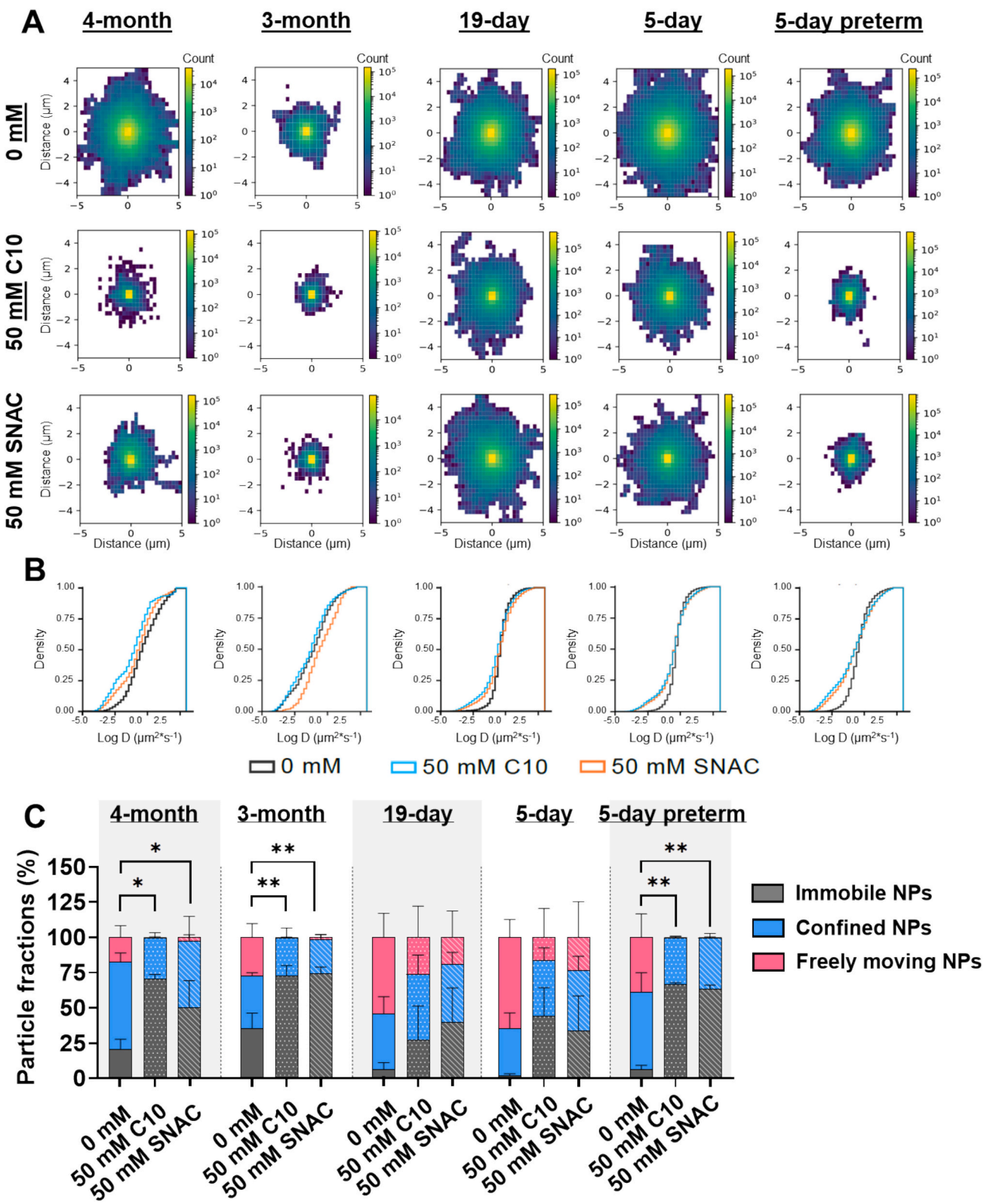

Fig. 3. Single particle tracking in *ex vivo* porcine small intestinal mucus collected from pigs of different ages and gestational maturities in the absence and the presence of 50 mM sodium decanoate (C10) or 50 mM sodium 8-[(2-hydroxybenzoyl)amino]octanoate (SNAC). A) 2D heatmaps of average nanoparticle (NP) coverage of 885–13,384 NPs in mucus collected from 4-month, 3-month, 19-day, and 5-day old pigs delivered via caesarean section either at term or preterm. B) accumulated densities of calculated diffusion coefficients (Log D) in mucus. C) stacked NP fractions of immobile NPs with $\alpha < 0.001$, confined NPs with $0.001 < \alpha < 0.5$ and freely moving NPs with $\alpha > 0.5$ in mucus. Data are given as a mean of biological replicates with standard deviation of $N = 3$, $n = 5$–10. The freely moving NP fraction was statistically different from the 0 mM condition for the C10 or SNAC group as stated by * ($p < 0.05$), ** ($p < 0.01$), *** ($p < 0.001$) or **** ($p < 0.0001$).

glycoprotein, and SA (i.e. sialic acid) contents of mucus to elucidate whether these physicochemical properties could account for the observed age- and gestational maturity-dependent effects of C10 and SNAC in mucus.

Interestingly, only the osmolality and protein content of mucus showed age-dependent differences (Fig. 4), with increasing age resulting in a decreased osmolality of 66% and an increased protein content of 43% when comparing 4-month and 5-day old pigs (Fig. 4B and C). In contrast, only the amount of SA in mucus was dependent on pig gestational maturity, with higher content in mature pigs (i.e. 5-day old pigs delivered at term (Fig. 4E)).

As mucins are the core structural backbone in mucus [9,10], we also investigated whether the expression of three different *MUC* genes in the small intestinal tissue showed age- and gestational maturity-dependent effects. Indeed, the relative gene expressions of the membrane-bound *MUC1* and the gel-forming *MUC2* and *MUC5AC* were lower in the younger pigs (i.e. 70–73% for 5-day and 75–94% for 19-day old pigs, respectively) compared to the 3-month old pigs, whereas the *MUC*-gene expression level was independent of pig gestational maturity (Fig. 4 G, Supplementary Material, Fig. S10). Interestingly, the age-related differences observed for *MUC2* and *MUC5AC* expression (Fig. 4G) were not reflected in the glycoprotein content of mucus (Fig. 4D), though this may be due to the presence of alternative non-mucin glycoproteins.

Overall, several physicochemical properties of mucus and *MUC*-gene expressions showed age-dependent effects, whereas this was not the case for gestational maturity. Only the total amount of SA in mucus had a dependency on the pig gestational maturity. In fact, the total amount of SA tended to be lower in mucus samples where C10 and SNAC effects were more pronounced (Fig. 3 and 4D). Hence, the SA content in mucus may govern interactions with C10 and SNAC.

3.4. C10 and SNAC mucus effects are diminished upon cleavage of SA in mucus

Terminal SA on the mucin strands give mucins an overall negative charge at physiological pH [1,10]. These negatively charged residues

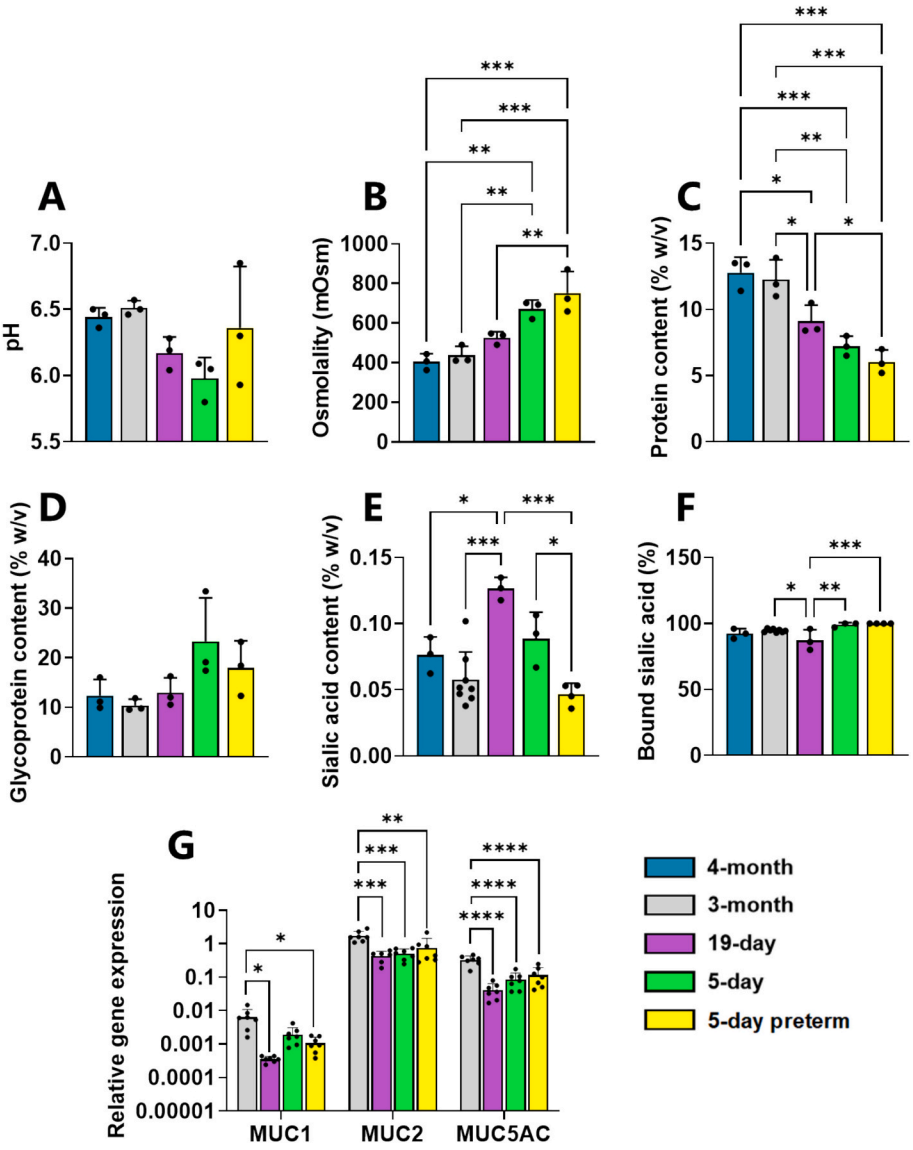

Fig. 4. Physicochemical properties of *ex vivo* porcine small intestinal mucus and mucin (*MUC*) gene expression in *ex vivo* porcine proximal small intestinal tissue. A) pH, B) osmolality, C) protein content, D) glycoprotein content, E) sialic acid content, and F) amount of bound sialic acid in mucus collected from pigs at different ages and gestational maturities ($N = 3$–8; $n = 1$–3). G) *MUC*-gene expressions in *ex vivo* porcine proximal small intestinal tissue collected from pigs at different ages and gestational maturities relative to the reference genes). Data are given as means with standard deviation of $N = 7$, $n = 2$. Individual biological replicates are marked by the black dots. Statistical significance between the different groups of pigs was indicated by * ($p < 0.05$), ** ($p < 0.01$) or *** ($p < 0.001$).

repel each other, which is important for the formation and gelation of the mucin network [10,44]. C10 and SNAC both carry a net negative charge at physiological pH [57], potentially affecting the electrostatic interactions between mucins and hence the mucus structure. To assess whether mucin-bound SA played a role in mucus's interaction with C10 and SNAC, terminal mucin-bound SA moieties were enzymatically cleaved using neuraminidase, and the viscoelastic properties of the isolated mucus pellet were assessed in the presence of C10 or SNAC (Fig. 5A).

As mucus is highly viscous, a minimum dilution of 4× was found necessary for the neuraminidase to cleave the terminal SA in mucus during 2 h incubation at 37 °C, being the optimal condition (Supplementary Material, Fig. S3B and C). This resulted in 41 ± 8% of the terminal SA in mucus being cleaved. Due to the presence of endogenous neuraminidases in mucus being capable of cleaving SA when incubated at 37 °C (Fig. 5A, B and Supplementary Material, Fig. S3C), we included an untreated mucus sample, which was not incubated at 37 °C (i.e. untreated÷). Total and free SA (i.e. TSA and FSA) contents were determined in the diluted mucus samples initially (i.e. 0 h), after 2 h of incubation at 37 °C, in the removed supernatants and in the collected mucus pellets (Fig. 5B). The amount of FSA after the 2 h incubation in neuraminidase-treated mucus was 2-fold higher compared to untreated-incubated mucus and 10-fold higher than the untreated÷ mucus sample (Fig. 6A). This indicated that the addition of exogenous

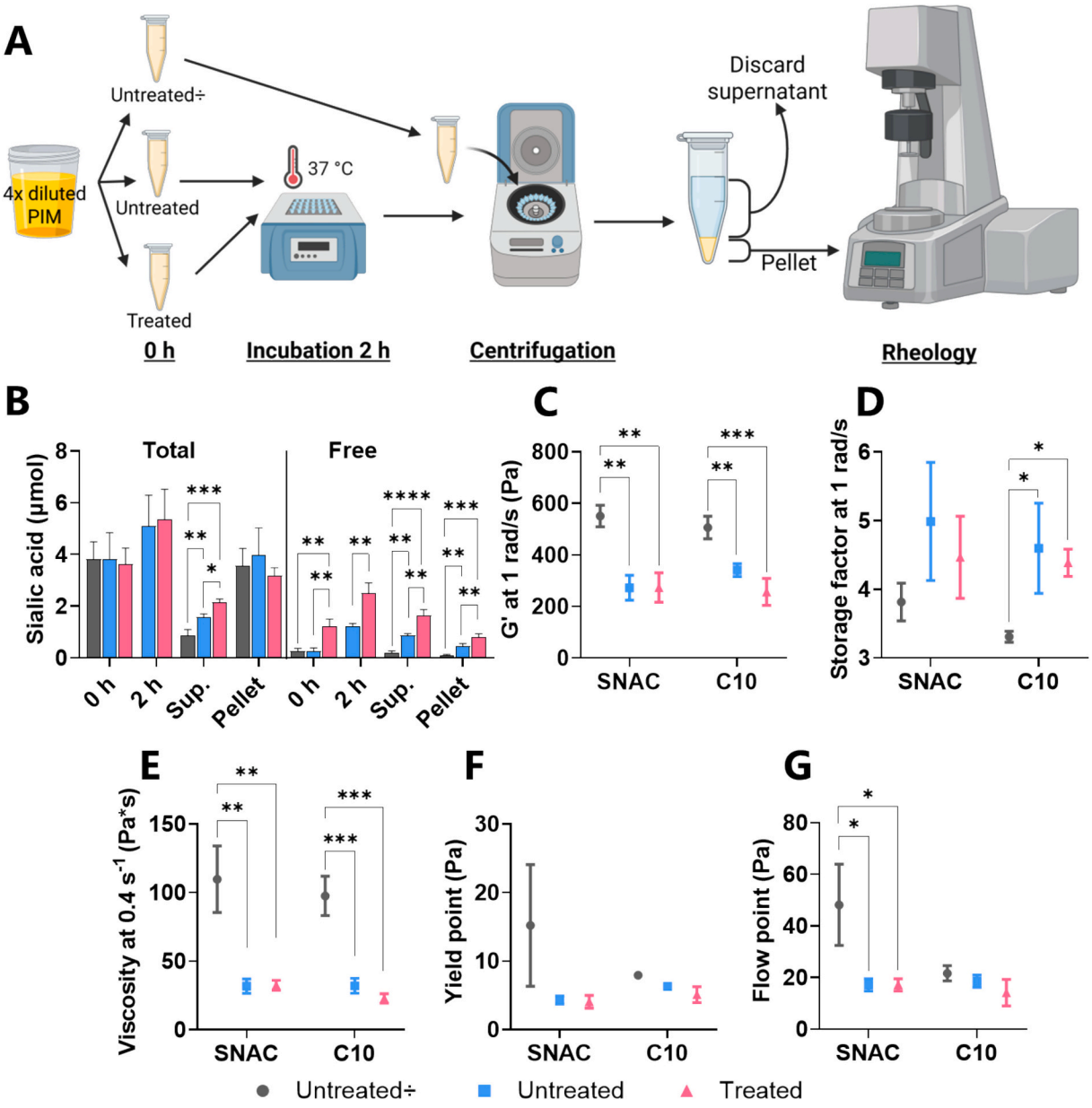

Fig. 5. Cleavage of sialic acid in *ex vivo* porcine small intestinal mucus (PIM) from 3 to 4-month old pigs and its effect on the viscoelastic properties of mucus pellets when in the presence of 150 mM sodium decanoate (C10) or 150 mM sodium 8-[(2-hydroxybenzoyl)amino]octanoate (SNAC). A) experimental schematics, B) amount of total and cleaved (i.e. free) sialic acid in untreated and neuraminidase-treated mucus after 0 and 2 h of incubation at 37 °C, discarded supernatant (Sup.) as well as in the pellet used for rheology. C) storage modulus (G′) at 1 rad/ s, D) storage factor (i.e. ratio of storage vs loss modulus (G′/G″) at 1 rad/s), E) viscosity at 0.4 s^{-1}, F) yield point (i.e. end of linear viscoelastic region, and G) flow point (i.e. G′ < G″ transition) of untreated and neuraminidase-treated mucus pellets in the presence of 150 mM C10 or SNAC. An untreated mucus sample without incubation (Untreated÷, grey circles) was included to account for the presence of endogenous enzymes in mucus able to cleave sialic acid upon incubation at 37 °C. Data are given as means of biological replicates with standard deviation of $N = 3$, $n = 1$–2. Data were statistically different between the different mucus samples as stated by * ($p < 0.05$), ** ($p < 0.01$), *** ($p < 0.001$) or **** ($p < 0.0001$).

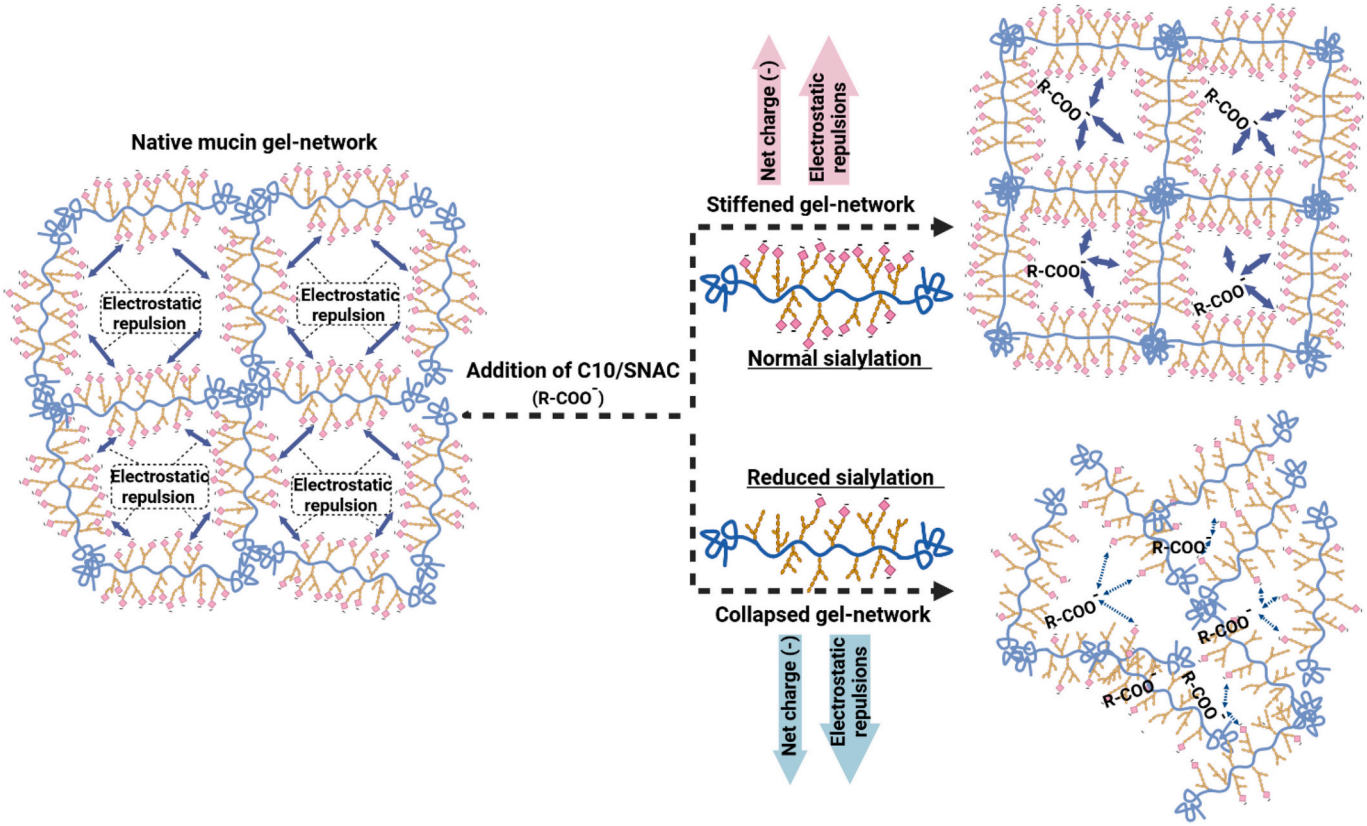

Fig. 6. Suggested mechanism by which sodium decanoate (C10) and sodium 8-[(2-hydroxybenzoyl)amino]octanoate (SNAC), both containing a terminal carboxylate group (R–COO⁻), modulate the mucin gel network. In native intestinal mucus, which has a high density of negatively charged terminal sialic acids on mucin strands, the additional negative charge from C10 and SNAC increases electrostatic repulsion, leading to a stiffened mucin gel network. In contrast, in mucus where terminal sialic acids have been cleaved, the overall negative charge is reduced, decreasing electrostatic repulsion between mucin-mucin or mucin-C10/SNAC, resulting in a more collapsed gel network.

neuraminidase was able to release more SA than the endogenous SA-cleaving enzymes. Despite all conditions initially containing the same amount of TSA, and more TSA was removed (i.e. supernatant, Fig. 5B) for the neuraminidase-treated sample compared to the untreated÷ and untreated-incubated samples, the TSA contents in the pellet samples tended to be the same for all conditions. Only the amount of FSA in the pellet samples differed, with 0.11, 0.47 and 0.80 μmol FSA in the untreated÷, untreated-incubated and neuraminidase-treated conditions, respectively.

Interestingly, when rheology was performed on the mucus pellets in the presence of the C10 or SNAC, no differences between the untreated-incubated and neuraminidase-treated mucus pellets were observed on any of the investigated rheological parameters (Fig. 5C-G, Supplementary Material, Fig. S2 for full rheological dataset). In contrast, all the rheological parameters for the untreated÷ pellet were significantly higher both in the presence of C10 and SNAC (Fig. 5C-G), suggesting that even the removal of a minor amount of SA or the presence of FSA in the mucus pellet significantly affected mucus' interaction with the C10 and SNAC. The decreased G′ and increased storage factor (only statistically significant for C10) for the untreated-incubated and neuraminidase-treated pellets (Fig. 5C and D), suggest that C10 and SNAC may have fewer but stronger intermolecular interactions in mucus when some of the terminal SA was cleaved off. Also, the viscosity (Fig. 5E) and stress stability (Fig. 5F and G) of the mucus pellets in the presence of C10 or SNAC decreased upon cleavage of SA, corresponding well with observed fewer intermolecular interactions Fig. 5C. Similar to the mucus diffusion studies in Fig. 4, we observed no difference between C10 and SNAC presence for any of the assessed rheological properties of the pellets (Fig. 5B-F), suggesting that C10 and SNAC may have a similar interaction with SA. As C10 and SNAC both contain a terminal carboxylate group, it is suggested that electrostatic repulsions rather than hydrophobic or specific binding interactions, dominate their rheological impact of C10 and SNAC in mucus (Fig. 6). In SA-containing mucus, both C10 and SNAC increase electrostatic repulsion and thereby stiffen the gel network (increased G′ and viscosity (Fig. 5E-G)), whereas SA removal diminishes charge density and abolishes this effect. Overall, SA played an important role in the interaction between mucus and the MCFA C10 and the MCFA derivative SNAC.

4. Discussion

In this study, we demonstrate how the MCFA C10, a common food degradation product, and SNAC, an MCFA derivative, alter intestinal mucus microstructure and the diffusion of NPs (employed as a pathogen marker) in an age- and gestational maturity-dependent manner. We collected and characterized small intestinal mucus from pigs spanning early life (5- and 19-day old pigs) to young adulthood (3- and 4-month old pigs) and through physicochemical profiling of the mucus, detailed insight into C10's and SNAC's mechanisms of action in the mucus were obtained. Porcine small intestinal mucus was used as it closely resembles human small intestinal mucus in structure, viscoelasticity, and NP diffusivity [68–71], in addition to that pigs share strong gastrointestinal similarities with both human infants and adults [72–74]. Thus, it represents an appropriate model for studying the human gastrointestinal mucus barrier function across various life stages.

Due to the natural complexity of native mucus and the limitations of simplified mucin models [37,75], we used rheological measurements to probe SNAC and C10 interactions with mucus under physiologically

relevant conditions, providing indirect yet informative insight into the underlying molecular mechanisms through changes in mucus network properties [76]. The rheological analysis showed that as little as 50 mM C10 or SNAC markedly altered the mucus' viscoelasticity, significantly increasing its viscosity, and at this concentration, both molecules exerted comparable effects. Despite changes to the pH and osmolality of mucus in the presence of C10 and SNAC, the observed changes in mucus viscoelasticity cannot be explained solely by pH or osmolality effects, as comparable or larger shifts in these parameters have previously resulted in only minor rheological changes [37]. Hence, the magnitude of the observed rheological changes exceeds what can be attributed to pH or osmolality alone, indicating that mucus-C10 and mucus-SNAC interactions are the dominant drivers of the increased viscoelasticity. Notably, while increasing SNAC concentrations further enhanced the strength of the intermolecular interactions and the stress stability of the mucus gel-network, increasing C10 concentrations led to a weakening of the mucus gel-network, approaching levels observed for untreated mucus. This suggests that C10 strengthens the mucus structure until a threshold value and then disrupts this strengthening of the gel-network of mucus at higher concentrations. The structural differences of the two molecules likely explain this behavior. The results may thus suggest that the hydrophilic terminal of SNAC contribute to this molecule's interactions with the large number of available hydrophilic mucin glycans, even at high concentrations. In contrast, the hydrophobic and less bulky tail of C10 determine preferential interaction with the more limited number of hydrophobic domains in mucus [43,57,77] initially leading to a more rigid gel-network. However, as the accessible hydrophobic domains become saturated, higher C10 concentrations lead to weakened interactions and thus lower viscosity of the mucus.

Consistent with previous reports [3,4,37,70], small intestinal mucus exhibited a heterogeneous microstructure with a wide distribution of pore sizes, both in the absence and presence of C10 and SNAC (Fig. 2). In mucus alone, the diffusion of the pathogen marker (i.e. NPs) varied with donor pig age, with older pigs showing increased NP confinement, confirming earlier observations in porcine and rodent intestinal mucus [2,4,70]. In line with our earlier work [3], gestational maturity (i.e. term) was also associated with increased pathogen marker diffusion. These age- and gestational maturity-dependent trends were expected to persist in the presence of C10 and SNAC. Although the presence of 50 mM C10 or SNAC induced a similar reduction in the diffusion of the pathogen marker within the same mucus group, the extent of confinement of the pathogen marker increased with the age and gestational immaturity of the pigs. Herein, we used 100–300 nm fluorescent polystyrene NPs to probe the passive barrier properties of mucus at the submicron scale [4,15,17,70,78] and while negatively charged and representative of many pathogens, these particles primarily model submicron-sized pathogenic species. As these 100–300 nm NPs already were largely immobilized or confined in the presence of C10 and SNAC, larger micron-sized NPs, modeling the size of pathogenic bacteria, would likely be largely immobilized or confined in mucus alone as previously reported [4,15,70,78] and therefore not provide additional insight into C10- or SNAC-induced changes in mucus barrier properties. Overall, our findings indicate that age and gestational maturity strongly modulate how intestinal mucus interacts and is affected by exogenous compounds such as C10 and SNAC.

Alterations to the physicochemical properties of mucus (e.g. pH, osmolality, mucin, and non-mucin constituents) are known to influence mucus structure and function [4,9,11,37,43]. We therefore hypothesized that the age- and gestational maturity-dependent effects of C10 and SNAC would be due to differences in the physicochemical properties of mucus. Several physicochemical properties of mucus and *MUC*-gene expressions showed clear age-dependent changes, whereas only the total SA content (i.e. TSA) varied with gestational maturity. Notably, TSA tended to be lower in mucus samples in which the effects of C10 and SNAC were most pronounced. Terminal mucin-bound SA give mucin their highly negative charge and is a key determinant of mucus' gel-network structure, viscoelasticity, and microbial trapping [9,45,46,79]. However, the role of SA in mucus' interactions with lipids, MCFA and derivatives such as C10 and SNAC remains poorly understood. Following the SA cleavage in mucus, the effects of C10 and SNAC on mucus elasticity and viscosity were markedly reduced, indicating a key role for terminal mucin-SA in relation to these compounds' interaction with mucus. Interestingly, these effects were equally reduced in C10 and SNAC presence, indicating that the observed rheological effects arise primarily from electrostatic contributions at the network level rather than specific binding interactions. In SA-containing mucus, the addition of negatively charged C10 and SNAC [43,57,77] enhances electrostatic repulsion within the mucin network, leading to mucin chain extension, increased entanglement, and reduced chain mobility, which manifests as increased G' and viscosity. Upon enzymatic removal of SA, the overall charge density of the mucin network is significantly reduced, thereby diminishing these electrostatic contributions. As a result, the incorporation of C10 and SNAC no longer induces the same degree of network stiffening. Importantly, removal of SA would also be expected to increase the accessibility of hydrophobic domains, potentially facilitating insertion of both C10 and SNAC into the mucin matrix [9,45,46,79]. However, C10, with its linear hydrophobic alkyl chain, is more likely to partition into hydrophobic domains of the mucin protein core than SNAC [43,57,77], and since both C10 and SNAC show a similar reduction in interaction after SA removal, this suggests that hydrophobic interactions do not significantly contribute to the macroscopic rheological properties. Notably, the extent of SA cleavage did not further affect C10's or SNAC's influence on the viscoelastic properties of the mucus. However, whether this arises from cleavage of SA or the presence of free SA requires further investigation. Additionally, while we used a neuraminidase with broad specificity, future studies using more specific neuraminidases may help resolve which SA moieties are most critical for mucus' interaction with MCFA and derivatives.

Overall, we showed that the MCFA, C10, and the synthetic derivative, SNAC, interacted with and altered small intestinal mucus in an age- and gestational maturity-dependent manner. Terminal mucin-bound SA emerged as a key modulator of these interactions, providing new insight into how MCFA- and derivative–mucus interactions evolve across life stages. Because mucin glycosylation and degree of sialylation [2,7,8,46,47,79] are altered by age and disease, the use of MCFAs and derivatives such as C10 and SNAC as nutritional supplements or pharmaceutical excipients, may result in substantial interindividual variability. Additionally, while the present study focuses on acute (1 h) *ex vivo* interactions between SNAC or C10 and mucus, it is important to note that SNAC and C10 administered daily for 21–28 days have been reported to alter the gut microbiota composition in vivo, which may indirectly influence mucus barrier properties [26,80]. Although most lipid–mucin interactions occur via hydrophobic mucin domains and many lipids lack a negative charge [9,10,43,77], SA may still indirectly modulate lipid-mucin association by altering mucin conformation, thereby exposing or shielding hydrophobic regions and stabilizing lipid interactions within the mucus gel-network.

5. Conclusion

This study demonstrates that the MCFA, C10, and the MCFA derivative, SNAC, modulate small intestinal mucus in an age- and gestation-dependent manner, with mucin-bound sialic acids playing a central role in these interactions. As little as 50 mM of either compound markedly increased mucus' viscosity and storage modulus G', with comparable effects at this concentration. While increasing concentrations of SNAC further strengthened the gel-network of mucus, C10 only strengthened mucus' gel-network at low concentrations but disrupted the gel-network beyond a threshold concentration. Importantly, the presence of C10 or SNAC significantly reduced the diffusion of pathogen-sized nanoparticles in mucus, with comparable effects within each mucus group, yet the magnitude of pathogen confinement increased with donor age

and gestational immaturity. Several physicochemical properties and *MUC-gene* expressions changed with age, while only the sialic acid content in mucus varied with gestational maturity. Notably, we found that removing terminal mucin-bound sialic acids weakened the C10 and SNAC induced changes to the viscoelastic properties of mucus, underscoring terminal mucin-bound sialic acid as a key factor of MCFA's and derivative's interactions with mucus across life stages. Overall, our results demonstrate that mucus barrier properties and the protective effects of C10 and SNAC vary significantly with age and gestational maturity, underscoring the need for age-specific nutritional and therapeutic strategies to support optimal gut health.

CRediT authorship contribution statement

J.S. Mortensen: Writing – review & editing, Writing – original draft, Visualization, Validation, Project administration, Methodology, Investigation, Formal analysis, Conceptualization. **L.S. Krog:** Writing – review & editing, Validation, Investigation, Formal analysis. **S.S.-R. Bohr:** Writing – review & editing, Visualization, Validation, Software, Methodology, Investigation, Formal analysis. **L. Råberg:** Writing – review & editing, Validation, Methodology, Investigation. **A. Stubelius:** Writing – review & editing, Supervision, Resources, Funding acquisition. **L. Saaby:** Writing – review & editing, Supervision. **N.S. Hatzakis:** Writing – review & editing, Supervision, Resources, Funding acquisition. **D.N. Nguyen:** Writing – review & editing, Supervision, Resources. **S. Rønholt:** Writing – review & editing, Supervision, Resources, Funding acquisition. **H.M. Nielsen:** Writing – review & editing, Supervision, Resources, Funding acquisition.

Declaration of Generative AI and AI-assisted technologies in the writing process

During the preparation of this work the authors used Microsoft 365 Copilot (version 19.2601.50081.0) to selectively improve language, clarity, and grammar. After using this tool, the authors reviewed and edited the content as needed and take full responsibility for the content of the publication.

Declaration of competing interest

The authors declare that they have no known competing financial interests or personal relationships that could have appeared to influence the work reported in this paper.

Acknowledgement

The Department of Experimental Medicine (University of Copenhagen) is greatly acknowledged for providing pig intestines. Johan Bøtker is acknowledged for his help analyzing the cryo-SEM images. This work was supported by the Novo Nordisk Foundation [NNF16OC0021948, NNF23OC0081287, and NNF22OC0075851], the Lundbeck Foundation, the Innovative Medicines Initiative Joint Undertaking [FP7/2007-2013 and EFPIA: 115363], the Carlsberg Foundation and the NordForsk [Nordic University Hub project #85352].

Appendix A. Supplementary data

Supplementary data to this article can be found online at https://doi.org/10.1016/j.ijbiomac.2026.154076.

Data availability

Data will be made available on request.

References

[1] J.K. Gustafsson, M.E.V. Johansson, The role of goblet cells and mucus in intestinal homeostasis, Nat. Rev. Gastroenterol. Hepatol. 19 (2022) 785–803, https://doi.org/10.1038/s41575-022-00675-x.
[2] J.Y. Lock, T.L. Carlson, Y. Yu, J. Lu, E.C. Claud, R.L. Carrier, Impact of developmental age, necrotizing enterocolitis associated stress, and oral therapeutic intervention on mucus barrier properties, Sci. Rep. 10 (2020) 6692, https://doi.org/10.1038/s41598-020-63593-5.
[3] J.S. Mortensen, S.S.R. Bohr, L.S. Krog, J.P. Bøtker, V. Kapousidou, L. Saaby, N. S. Hatzakis, H.M. Nielsen, D.N. Nguyen, S. Rønholt, Neonatal intestinal mucus barrier changes in response to maturity, inflammation, and sodium decanoate supplementation, Sci. Rep. 14 (2024) 7665, https://doi.org/10.1038/s41598-024-58356-5.
[4] A. Macierzanka, A.R. Mackie, B.H. Bajka, N.M. Rigby, F. Nau, D. Dupont, Transport of particles in intestinal mucus under simulated infant and adult physiological conditions: impact of mucus structure and extracellular DNA, PLoS One 9 (2014) e95274, https://doi.org/10.1371/journal.pone.0095274.
[5] M.E.V. Johansson, Mucus layers in inflammatory bowel disease, Inflamm. Bowel Dis. 20 (2014) 2124–2131, https://doi.org/10.1097/mib.0000000000000117.
[6] M.E.V. Johansson, H. Sjövall, G.C. Hansson, The gastrointestinal mucus system in health and disease, Nat. Rev. Gastroenterol. Hepatol. 10 (2013) 352–361, https://doi.org/10.1038/nrgastro.2013.35.
[7] X. Sang, Q. Wang, Y. Ning, H. Wang, R. Zhang, Y. Li, B. Fang, C. Lv, Y. Zhang, X. Wang, F. Ren, Age-related mucus barrier dysfunction in mice is related to the changes in Muc2 mucin in the colon, Nutrients 15 (2023) 1830, https://doi.org/10.3390/nu15081830.
[8] J.M.H. Larsson, H. Karlsson, J.G. Crespo, M.E.V. Johansson, L. Eklund, H. Sjövall, G.C. Hansson, Altered O-glycosylation profile of MUC2 mucin occurs in active ulcerative colitis and is associated with increased inflammation, Inflamm. Bowel Dis. 17 (2011) 2299–2307, https://doi.org/10.1002/ibd.21625.
[9] J. Leal, H.D.C. Smyth, D. Ghosh, Physicochemical properties of mucus and their impact on transmucosal drug delivery, Int. J. Pharm. 532 (2017) 555–572, https://doi.org/10.1016/j.ijpharm.2017.09.018.
[10] R. Bansil, B.S. Turner, The biology of mucus: composition, synthesis and organization, Adv. Drug Deliv. Rev. 124 (2018) 3–15, https://doi.org/10.1016/j.addr.2017.09.023.
[11] V.L.N. Murty, J. Sarosiek, A. Slomiany, B.L. Slomiany, Effect of lipids and proteins on the viscosity of gastric mucus glycoprotein, Biochem. Biophys. Res. Commun. 121 (1984) 521–529, https://doi.org/10.1016/0006-291X(84)90213-4.
[12] A. Braun, W. Stremmel, R. Ehehalt, The role of phospholipids within the intestinal mucosal barrier, Z. Gastroenterol. 49 (2011) A11, https://doi.org/10.1055/s-0031-1304771.
[13] A. Braun, I. Treede, D. Gotthardt, A. Tietje, A. Zahn, R. Ruhwald, U. Schoenfeld, T. Welsch, P. Kienle, G. Erben, W.D. Lehmann, J. Fuellekrug, W. Stremmel, R. Ehehalt, Alterations of phospholipid concentration and species composition of the intestinal mucus barrier in ulcerative colitis: a clue to pathogenesis, Inflamm. Bowel Dis. 15 (2009) 1705–1720, https://doi.org/10.1002/ibd.20993.
[14] T.L. Carlson, H. Yildiz, Z. Dar, J.Y. Lock, R.L. Carrier, Lipids alter microbial transport through intestinal mucus, PLoS One 13 (2018) e0209151, https://doi.org/10.1371/journal.pone.0209151.
[15] H.M. Yildiz, C.A. McKelvey, P.J. Marsac, R.L. Carrier, Size selectivity of intestinal mucus to diffusing particulates is dependent on surface chemistry and exposure to lipids, J. Drug Target. 23 (2015) 768–774, https://doi.org/10.3109/1061186X.2015.1086359.
[16] H.M. Yildiz, L. Speciner, C. Ozdemir, D.E. Cohen, R.L. Carrier, Food-associated stimuli enhance barrier properties of gastrointestinal mucus, Biomaterials 54 (2015) 1–8, https://doi.org/10.1016/j.biomaterials.2015.02.118.
[17] J.Y. Lock, T.L. Carlson, C.M. Wang, A. Chen, R.L. Carrier, Acute exposure to commonly ingested emulsifiers alters intestinal mucus structure and transport properties, Sci. Rep. 8 (2018) 10008, https://doi.org/10.1038/s41598-018-27957-2.
[18] B. Delplanque, R. Gibson, B. Koletzko, A. Lapillonne, B. Strandvik, Lipid quality in infant nutrition: current knowledge and future opportunities, J. Pediatr. Gastroenterol. Nutr. 61 (2015) 8–17, https://doi.org/10.1097/mpg.0000000000000818.
[19] M.A. Mendonça, W.M.C. Araújo, L.A. Borgo, E.R. Alencar, Lipid profile of different infant formulas for infants, PLoS One 12 (2017) e0177812, https://doi.org/10.1371/journal.pone.0177812.
[20] G. Roda, S. Fialà, M. Vittorini, F. Secundo, Fatty acid composition and fat content in milk from cows grazing in the Alpine region, Eur. Food Res. Technol. 241 (2015) 413–418, https://doi.org/10.1007/s00217-015-2473-3.
[21] D. Mota-Rojas, D. Villanueva-García, A. Solimano, R. Muns, D. Ibarra-Ríos, A. Mota-Reyes, Pathophysiology of perinatal asphyxia in humans and animal models, Biomedicines 10 (2022) 347, https://doi.org/10.3390/biomedicines10020347.
[22] A.T. Rose, R.M. Patel, A critical analysis of risk factors for necrotizing enterocolitis, Semin. Fetal Neonatal Med. 23 (2018) 374–379, https://doi.org/10.1016/j.siny.2018.07.005.
[23] J. Neu, W.A. Walker, Necrotizing enterocolitis, N. Engl. J. Med. 364 (2011) 255–264, https://doi.org/10.1056/NEJMra1005408.
[24] T.R. Thänert, E.C. Keen, G. Dantas, B.B. Warner, P.I. Tarr, Necrotizing enterocolitis and the microbiome: current status and future directions, J. Infect. Dis. 223 (2021) S257–s63, https://doi.org/10.1093/infdis/jiaa604.
[25] J.A. Jackman, R.D. Boyd, C. C Elrod, Medium-chain fatty acids and monoglycerides as feed additives for pig production: towards gut health improvement and feed

pathogen mitigation, J. Anim. Sci. Biotechnol. 11 (2020) 44, https://doi.org/10.1186/s40104-020-00446-1.
[26] J. Zhao, J. Hu, X. Ma, Sodium decanoate improves intestinal epithelial barrier and antioxidation via activating G protein-coupled receptor-43, Nutrients 13 (2021) 2756, https://doi.org/10.3390/nu13082756.
[27] B. Wang, L. Li, J. Fu, P. Yu, D. Gong, C. Zeng, Z. Zeng, Effects of long-chain and medium-chain fatty acids on apoptosis and oxidative stress in human liver cells with steatosis, J. Food Sci. 81 (2016) H794–H800, https://doi.org/10.1111/1750-3841.13210.
[28] Food Additive Status List: U.S. Food & Drug Administration. https://www.fda.gov/food/food-additives-petitions/food-additive-status-list#abb, 2022. (Accessed 12 January 2026).
[29] EFSA Panel on Food Additives and Nutrient Sources added to Food, A. Mortensen, F. Aguilar, R. Crebelli, A. Di Domenico, B. Dusemund, M.J. Frutos, P. Galtier, D. Gott, U. Gundert-Remy, J.C. Leblanc, O. Lindtner, P. Moldeus, P. Mosesso, D. Parent-Massin, A. Oskarsson, I. Stankovic, I. Waalkens-Berendsen, R. A. Woutersen, M. Wright, M. Younes, P. Boon, D. Chrysafidis, R. Gürtler, P. Tobback, P. Gergelova, A.M. Rincon, C. Lambré, Re-evaluation of fatty acids (E 570) as a food additive, EFSA J. 15 (2017) e04785, https://doi.org/10.2903/j.efsa.2017.4785.
[30] M. Younes, P. Aggett, F. Aguilar, R. Crebelli, B. Dusemund, M. Filipič, M.J. Frutos, P. Galtier, D. Gott, U. Gundert-Remy, G.G. Kuhnle, J.C. Leblanc, I.T. Lillegaard, P. Moldeus, A. Mortensen, A. Oskarsson, I. Stankovic, I. Waalkens-Berendsen, R. A. Woutersen, M. Wright, P. Boon, D. Chrysafidis, R. Gürtler, P. Mosesso, D. Parent-Massin, P. Tobback, C. Cascio, A.M. Rincon, C. Lambré, Re-evaluation of sodium, potassium and calcium salts of fatty acids (E 470a) and magnesium salts of fatty acids (E 470b) as food additives, EFSA J. 16 (2018) e05180, https://doi.org/10.2903/j.efsa.2018.5180.
[31] S. Maher, D.J. Brayden, L. Casettari, L. Illum, Application of permeation enhancers in oral delivery of macromolecules: an update, Pharmaceutics 11 (2019) 41, https://doi.org/10.3390/pharmaceutics11010041.
[32] D.J. Brayden, T.A. Hill, D.P. Fairlie, S. Maher, R.J. Mrsny, Systemic delivery of peptides by the oral route: formulation and medicinal chemistry approaches, Adv. Drug Deliv. Rev. 157 (2020) 2–36, https://doi.org/10.1016/j.addr.2020.05.007.
[33] M. Bohley, J.C. Leroux, Gastrointestinal permeation enhancers beyond sodium caprate and SNAC - what is coming next? Adv. Sci. (Weinh) 11 (2024) e2400843 https://doi.org/10.1002/advs.202400843.
[34] S.T. Buckley, T.A. Baekdal, A. Vegge, S.J. Maarbjerg, C. Pyke, J. Ahnfelt-Ronne, K. G. Madsen, S.G. Scheele, T. Alanentalo, R.K. Kirk, B.L. Pedersen, R.B. Skyggebjerg, A.J. Benie, H.M. Strauss, P.O. Wahlund, S. Bjerregaard, E. Farkas, C. Fekete, F. L. Sondergaard, J. Borregaard, M.L. Hartoft-Nielsen, L.B. Knudsen, Transcellular stomach absorption of a derivatized glucagon-like peptide-1 receptor agonist, Sci. Transl. Med. 10 (2018) 467, https://doi.org/10.1126/scitranslmed.aar7047.
[35] RYBELSUS® (semaglutide) Tablets for Oral Use, U.S. Food and Drug Administration, 2019. https://www.accessdata.fda.gov/drugsatfda_docs/label/2019/213051s000lbl.pdf. (Accessed 12 January 2026).
[36] C. Twarog, F. McCartney, S.M. Harrison, B. Illel, E. Fattal, D.J. Brayden, Comparison of the effects of the intestinal permeation enhancers, SNAC and sodium caprate (C(10)): isolated rat intestinal mucosae and sacs, Eur. J. Pharm. Sci. 158 (2021) 105685, https://doi.org/10.1016/j.ejps.2020.105685.
[37] J.S. Mortensen, S.S.R. Bohr, S. Harloff-Helleberg, N.S. Hatzakis, L. Saaby, H. M. Nielsen, Physical and barrier changes in gastrointestinal mucus induced by the permeation enhancer sodium 8-[(2-hydroxybenzoyl)amino]octanoate (SNAC), J. Control. Release 352 (2022) 163–178, https://doi.org/10.1016/j.jconrel.2022.09.034.
[38] R.D. Pullan, G.A. Thomas, M. Rhodes, R.G. Newcombe, G.T. Williams, A. Allen, J. Rhodes, Thickness of adherent mucus gel on colonic mucosa in humans and its relevance to colitis, Gut 35 (1994) 353–359, https://doi.org/10.1136/gut.35.3.353.
[39] N. Baidoo, G.J. Sanger, Age-related decline in goblet cell numbers and mucin content of the human colon: implications for lower bowel functions in the elderly, Exp. Mol. Pathol. 139 (2024) 104923, https://doi.org/10.1016/j.yexmp.2024.104923.
[40] M. Elderman, B. Sovran, F. Hugenholtz, K. Graversen, M. Huijskes, E. Houtsma, C. Belzer, M. Boekschoten, P. de Vos, J. Dekker, J. Wells, M. Faas, The effect of age on the intestinal mucus thickness, microbiota composition and immunity in relation to sex in mice, PLoS One 12 (2017) e0184274-e, https://doi.org/10.1371/journal.pone.0184274.
[41] J. Dekker, W.M.O. Van Beurden-Lamers, A. Oprins, G.J. Strous, Isolation and structural analysis of rat gastric mucus glycoprotein suggests a homogeneous protein backbone, Biochem. J. 260 (1989) 717–723, https://doi.org/10.1042/bj2600717.
[42] I. Brockhausen, Sulphotransferases acting on mucin-type oligosaccharides, Biochem. Soc. Trans. 31 (2003) 318–325, https://doi.org/10.1042/bst0310318.
[43] T.L. Carlson, J.Y. Lock, R.L. Carrier, Engineering the mucus barrier, Annu. Rev. Biomed. Eng. 20 (2018) 197–220, https://doi.org/10.1146/annurev-bioeng-062117-121156.
[44] J.S. Mortensen, M.B. Stie, S. Harloff-Helleberg, H.M. Nielsen, Overcoming the mucus barrier, in: L.S. Milane, M.M. Amiji (Eds.), Organelle and Molecular Targeting, 1st ed., CRC Press, Boca Raton, 2021, pp. 355–379, https://doi.org/10.1201/9781003092773-14.
[45] T.S. Raju, E.A. Davidson, Role of sialic acid on the viscosity of canine tracheal mucin glycoprotein, Biochem. Biophys. Res. Commun. 205 (1994) 402–409, https://doi.org/10.1006/bbrc.1994.2679.
[46] M. Taniguchi, R. Okumura, T. Matsuzaki, A. Nakatani, K. Sakaki, S. Okamoto, A. Ishibashi, H. Tani, M. Horikiri, N. Kobayashi, H.Y. Yoshikawa, D. Motooka, D. Okuzaki, S. Nakamura, T. Kida, A. Kameyama, K. Takeda, Sialylation shapes mucus architecture inhibiting bacterial invasion in the colon, Mucosal Immunol. 16 (2023) 624–641, https://doi.org/10.1016/j.mucimm.2023.06.004.
[47] M. Matsuzawa, T. Ando, S. Fukase, M. Kimura, Y. Kume, T. Ide, K. Izawa, A. Kaitani, M. Hara, E. Nakamura, A. Kamei, A. Matsuda, N. Nakano, K. Maeda, N. Tada, H. Ogawa, K. Okumura, A. Murakami, N. Ebihara, J. Kitaura, The protective role of conjunctival goblet cell mucin sialylation, Nat. Commun. 14 (2023) 1417, https://doi.org/10.1038/s41467-023-37101-y.
[48] C. de Loubens, R.G. Lentle, R.J. Love, C. Hulls, P.W. Janssen, Fluid mechanical consequences of pendular activity, segmentation and pyloric outflow in the proximal duodenum of the rat and the guinea pig, J. R. Soc. Interface 10 (2013) 20130027, https://doi.org/10.1098/rsif.2013.0027.
[49] F. Wan, S.S.R. Bohr, S.N. Kłodzińska, H. Jumaa, Z. Huang, T. Nylander, M. B. Thygesen, K.K. Sørensen, K.J. Jensen, C. Sternberg, N.S. Hatzakis, H.M. Nielsen, Ultrasmall TPGS–PLGA hybrid nanoparticles for site-specific delivery of antibiotics into *Pseudomonas aeruginosa* biofilms in lungs, ACS Appl. Mater. Interfaces 12 (2020) 380–389, https://doi.org/10.1021/acsami.9b19644.
[50] S.S.R. Bohr, P.M. Lund, A.S. Kallenbach, H.D. Pinholt, J. Thomsen, L. Iversen, A. Svendsen, S.M. Christensen, N.S. Hatzakis, Direct observation of *Thermomyces lanuginosus* lipase diffusional states by single particle tracking and their remodeling by mutations and inhibition, Sci. Rep. 9 (2019) 16169, https://doi.org/10.1038/s41598-019-52539-1.
[51] H.D. Pinholt, S.S.R. Bohr, J.F. Iversen, W. Boomsma, N.S. Hatzakis, Single-particle diffusional fingerprinting: a machine-learning framework for quantitative analysis of heterogeneous diffusion, Proc. Natl. Acad. Sci. USA 118 (2021) e2104624118, https://doi.org/10.1073/pnas.2104624118.
[52] S. Streck, S.S.R. Bohr, D. Birch, T. Rades, N.S. Hatzakis, A. McDowell, H.M. Nielsen, Interactions of cell-penetrating peptide-modified nanoparticles with cells evaluated using single particle tracking, ACS Appl. Bio Mater. 4 (2021) 3155–3165, https://doi.org/10.1021/acsabm.0c01563.
[53] M.E. Moses, P.M. Lund, S.S.R. Bohr, J.F. Iversen, J. Kæstel-Hansen, A. S. Kallenbach, L. Iversen, S.M. Christensen, N.S. Hatzakis, Single-molecule study of thermomyces lanuginosus lipase in a detergency application system reveals diffusion pattern remodeling by surfactants and calcium, ACS Appl. Mater. Interfaces 13 (2021) 33704–33712, https://doi.org/10.1021/acsami.1c08809.
[54] B.C. Huck, O. Hartwig, A. Biehl, K. Schwarzkopf, C. Wagner, B. Loretz, X. Murgia, C.M. Lehr, Macro- and microrheological properties of mucus surrogates in comparison to native intestinal and pulmonary mucus, Biomacromolecules 20 (2019) 3504–3512, https://doi.org/10.1021/acs.biomac.9b00780.
[55] M. Kilcoyne, J.Q. Gerlach, M.P. Farrell, V.P. Bhavanandan, L. Joshi, Periodic acid-Schiff's reagent assay for carbohydrates in a microtiter plate format, Anal. Biochem. 416 (2011) 18–26, https://doi.org/10.1016/j.ab.2011.05.006.
[56] J.S. Mortensen, L. Saaby, S. Harloff-Helleberg, H.M. Nielsen, Barrier properties of *ex vivo* porcine intestinal mucus are highly independent of isolation and storage conditions, Eur. J. Pharm. Biopharm. 174 (2022) 106–110, https://doi.org/10.1016/j.ejpb.2022.03.015.
[57] C. Twarog, S. Fattah, J. Heade, S. Maher, E. Fattal, D.J. Brayden, Intestinal permeation enhancers for oral delivery of macromolecules: a comparison between salcaprozate sodium (SNAC) and sodium caprate (C10), Pharmaceutics 11 (2019) 78, https://doi.org/10.3390/pharmaceutics11020078.
[58] D. Birch, R.G. Diedrichsen, P.C. Christophersen, H. Mu, H.M. Nielsen, Evaluation of drug permeation under fed state conditions using mucus-covered Caco-2 cell epithelium, Eur. J. Pharm. Sci. 118 (2018) 144–153, https://doi.org/10.1016/j.ejps.2018.02.032.
[59] C. Twarog, K. Liu, P.J. O'Brien, K.A. Dawson, E. Fattal, B. Illel, D.J. Brayden, A head-to-head Caco-2 assay comparison of the mechanisms of action of the intestinal permeation enhancers: SNAC and sodium caprate (C10), Eur. J. Pharm. Biopharm. 152 (2020) 95–107, https://doi.org/10.1016/j.ejpb.2020.04.023.
[60] M. Baluom, M. Friedman, A. Rubinstein, The importance of intestinal residence time of absorption enhancer on drug absorption and implication on formulative considerations, Int. J. Pharm. 176 (1998) 21–30, https://doi.org/10.1016/S0378-5173(98)00288-9.
[61] S. Berg, L. Kärrberg, D. Suljovic, F. Seeliger, M. Söderberg, M. Perez-Alcazar, N. Van Zuydam, B. Abrahamsson, A.M. Hugerth, N. Davies, C.A.S. Bergström, Impact of intestinal concentration and colloidal structure on the permeation-enhancing efficiency of sodium caprate in the rat, Mol. Pharm. 19 (2022) 200–212, https://doi.org/10.1021/acs.molpharmaceut.1c00724.
[62] S. Berg, D. Suljovic, L. Kärrberg, M. Englund, H. Bönisch, I. Karlberg, N. Van Zuydam, B. Abrahamsson, A.M. Hugerth, N. Davies, C.A.S. Bergström, Intestinal absorption of fITC-dextrans and macromolecular model drugs in the rat intestinal instillation model, Mol. Pharm. 19 (2022) 2564–2572, https://doi.org/10.1021/acs.molpharmaceut.2c00261.
[63] C. Solis-Herrera, M.P. Kane, C. Triplitt, Current understanding of sodium N-(8-[2-hydroxylbenzoyl] amino) caprylate (SNAC) as an absorption enhancer: the oral semaglutide experience, Clin. Diabetes 42 (2023) 74–86, https://doi.org/10.2337/cd22-0118.
[64] I.B. Halberg, K. Lyby, K. Wassermann, T. Heise, E. Zijlstra, L. Plum-Mörschel, Efficacy and safety of oral basal insulin versus subcutaneous insulin glargine in type 2 diabetes: a randomised, double-blind, phase 2 trial, Lancet Diabetes Endocrinol. 7 (2019) 179–188, https://doi.org/10.1016/S2213-8587(18)30372-3.
[65] Z. Vinarov, M. Abdallah, J.A.G. Agundez, K. Allegaert, A.W. Basit, M. Braeckmans, J. Ceulemans, M. Corsetti, B.T. Griffin, M. Grimm, D. Keszthelyi, M. Koziolek, C. M. Madla, C. Matthys, L.E. McCoubrey, A. Mitra, C. Reppas, J. Stappaerts, N. Steenackers, N.L. Trevaskis, T. Vanuytsel, M. Vertzoni, W. Weitschies, C. Wilson, P. Augustijns, Impact of gastrointestinal tract variability on oral drug absorption

and pharmacokinetics: an UNGAP review, Eur. J. Pharm. Sci. 162 (2021) 105812, https://doi.org/10.1016/j.ejps.2021.105812.
[66] J. Ceulemans, A. Ludwig, Optimisation of carbomer viscous eye drops: an in vitro experimental design approach using rheological techniques, Eur. J. Pharm. Biopharm. 54 (2002) 41–50, https://doi.org/10.1016/s0939-6411(02)00036-x.
[67] P.D. Cani, Human gut microbiome: hopes, threats and promises, Gut 67 (2018) 1716–1725, https://doi.org/10.1136/gutjnl-2018-316723.
[68] T. T Kararli, Comparison of the gastrointestinal anatomy, physiology, and biochemistry of humans and commonly used laboratory animals, Biopharm. Drug Dispos. 16 (1995) 351–380, https://doi.org/10.1002/bdd.2510160502.
[69] A.C. Groo, F. Lagarce, Mucus models to evaluate nanomedicines for diffusion, Drug Discov. Today 19 (2014) 1097–1108, https://doi.org/10.1016/j.drudis.2014.01.011.
[70] L. Krupa, B. Bajka, R. Staroń, D. Dupont, H. Singh, K. Gutkowski, A. Macierzanka, Comparing the permeability of human and porcine small intestinal mucus for particle transport studies, Sci. Rep. 10 (2020) 20290, https://doi.org/10.1038/s41598-020-77129-4.
[71] V. Barmpatsalou, I.R. Dubbelboer, A. Rodler, M. Jacobson, E. Karlsson, B. L. Pedersen, C.A.S. Bergström, Physiological properties, composition and structural profiling of porcine gastrointestinal mucus, Eur. J. Pharm. Biopharm. 169 (2021) 156–167, https://doi.org/10.1016/j.ejpb.2021.10.008.
[72] Q. Sciascia, G. Daş, C.C. Metges, The pig as a model for humans: effects of nutritional factors on intestinal function and health, J. Anim. Sci. 94 (2016) 441–452, https://doi.org/10.2527/jas.2015-9788.
[73] Q. Zhang, G. Widmer, S. Tzipori, A pig model of the human gastrointestinal tract, Gut Microbes 4 (2013) 193–200, https://doi.org/10.4161/gmic.23867.
[74] D. Burrin, P.T. Sangild, B. Stoll, T. Thymann, R. Buddington, J. Marini, O. Olutoye, R.J. Shulman, Translational advances in pediatric nutrition and gastroenterology: new insights from pig models, Annu. Rev. Anim. Biosci. 8 (2020) 321–354, https://doi.org/10.1146/annurev-animal-020518-115142.
[75] C.M. Wang, M.T. Fernez, B.M. Woolston, R.L. Carrier, Native gastrointestinal mucus: critical features and techniques for studying interactions with drugs, drug carriers, and bacteria, Adv. Drug Deliv. Rev. 200 (2023) 114966, https://doi.org/10.1016/j.addr.2023.114966.
[76] E. Nikoumanesh, C.J.M. Jouaneh, R. Poling-Skutvik, Elucidating the role of physicochemical interactions on gel rheology, Soft Matter 20 (2024) 7094–7102, https://doi.org/10.1039/D4SM00516C.
[77] C.V. Recktenwald, G. Karlsson, M.J. Garcia-Bonete, G. Katona, M. Jensen, R. Lymer, M. Bäckström, M.E.V. Johansson, G.C. Hansson, S. Trillo-Muyo, The structure of the second CysD domain of MUC2 and role in mucin organization by transglutaminase-based cross-linking, Cell Rep. 43 (2024) 114207, https://doi.org/10.1016/j.celrep.2024.114207.
[78] B.H. Bajka, N.M. Rigby, K.L. Cross, A. Macierzanka, A.R. Mackie, The influence of small intestinal mucus structure on particle transport ex vivo, Colloids Surf. B Biointerfaces 135 (2015) 73–80, https://doi.org/10.1016/j.colsurfb.2015.07.038.
[79] Y. Yao, G. Kim, S. Shafer, Z. Chen, S. Kubo, Y. Ji, J. Luo, W. Yang, S.P. Perner, C. Kanellopoulou, A.Y. Park, P. Jiang, J. Li, S. Baris, E.K. Aydiner, D. Ertem, D. J. Mulder, N. Warner, A.M. Griffiths, C. Topf-Olivestone, M. Kori, L. Werner, J. Ouahed, M. Field, C. Liu, B. Schwarz, C.M. Bosio, S. Ganesan, J. Song, H. Urlaub, T. Oellerich, S.A. Malaker, L. Zheng, C.R. Bertozzi, Y. Zhang, H. Matthews, W. Montgomery, H.Y. Shih, J. Jiang, M. Jones, A. Baras, A. Shuldiner, C. Gonzaga-Jauregui, S.B. Snapper, A.M. Muise, D.S. Shouval, A. Ozen, K.T. Pan, C. Wu, M. J. Lenardo, Mucus sialylation determines intestinal host-commensal homeostasis, Cell 185 (2022) 172–188, https://doi.org/10.1016/j.cell.2022.02.013.
[80] A. Ariaee, K. Noueihad, A. Hunter, A. Wignall, H.R. Wardill, M. Davies, C. A. Prestidge, P. Joyce, Gut microbiota perturbation and systemic inflammation are associated with salcaprozate sodium (SNAC)-enabled oral semaglutide delivery, J. Control. Release 392 (2026) 114711, https://doi.org/10.1016/j.jconrel.2026.114711.